Surface Properties of Superhydrophobic Coatings for Stone Protection

Ioannis Zuburtikudis

Journal of Nano Research

Surface Properties of Superhydrophobic Coatings for Stone Protection

Article *in* Journal of Nano Research · September 2009

DOI: 10.4028/www.scientific.net/JNanoR.8.23

Appl Phys A (2009) 97: 351–360
DOI 10.1007/s00339-009-5233-z

Applied Physics A
Materials Science & Processing

Superhydrophobic films for the protection of outdoor cultural heritage assets

P.N. Manoudis · I. Karapanagiotis · A. Tsakalof · I. Zuburtikudis · B. Kolinkeová · C. Panayiotou

Received: 22 December 2008 / Accepted: 15 April 2009 / Published online: 26 April 2009

Abstract A very simple method that can be used to impart superhydrophobicity to stone surfaces of monuments using common and low-cost materials that are already employed or are easy to be found by conservators is presented. A siloxane-nanoparticle dispersion is sprayed on a stone, and this process can result in the formation of a rough two-length-scale hierarchical structure that exhibits water repellent properties, provided that the nanoparticle concentration in the dispersion is higher than a critical value. Superhydrophobicity (static contact angle $>150°$ and contact angle hysteresis $<7°$) is achieved, by this simple method (i) on the surfaces of three types of stones, Opuka, Božanovský and Hořický, which have been used for the restoration of the castle of Prague, (ii) using two poly (alkyl siloxane) products such as Rhodorsil 224 and Porosil VV plus, which are utilized by conservators and (iii) using common nanoparticles such as silica (SiO_2), alumina (Al_2O_3), tin oxide (SnO_2) and titanium oxide (TiO_2). It is shown that the stone substrate and the nanoparticle size (5–50 nm) or type have almost no effect on the wettability of the superhydrophobic surfaces, as comparable contact angles were measured on the three stone substrates, treated with any siloxane-particle composite. Treatments of the stones with pure (hydrophobic) siloxanes and siloxane-SiO_2 (superhydrophobic) composites result in comparable reductions of the water vapor permeability and the water amounts absorbed by capillarity. Consequently, the use of nanoparticles in the protective coatings does not have any obvious effect on the results of the aforementioned tests. However, the aesthetic appearance of the three stones, included in this study, is highly affected by the nanoparticles.

PACS 68.35.Ct · 62.23.St · 96.12.kc · 81.15.Rs · 82.35.Np

P.N. Manoudis · B. Kolinkeová · C. Panayiotou
Department of Chemical Engineering, Aristotle University of Thessaloniki, 54124 Thessaloniki, Greece

I. Karapanagiotis (✉)
Art Diagnosis Centre, Ormylia Foundation, Ormylia, Chalkidiki 63071, Greece
e-mail: g.karapanagiotis@artdiagnosis.gr
Fax: +30-2371-098402

A. Tsakalof
Medical Department, University of Thessaly, 41222 Larissa, Greece

I. Zuburtikudis
Department of Industrial Design Engineering, TEI of Western Macedonia, 50100 Kozani, Greece

B. Kolinkeová
Department of Chemical Technology, Institute of Chemical Technology, (ICT Prague), 16628 Prague 6, Czech Republic

1 Introduction

In nature many plant surfaces, like for instance the leaves of *Nelumbo nucifera* Gaertn. (a divine symbol in Hindu tradition from ancient times), *Colocasia esculenta* L. (grown for its edible corm since antiquity) and *Cotinus Coggygria* Scop. (used for dyeing textiles since antiquity), exhibit enhanced water repellency which is attributed to their textured surfaces with hierarchical micrometer- and nanometer-sized structures in connection to hydrophobic surface components [1–4]. Interestingly, similar specially textured topographies were observed in the wings of some insects [5–7]. In the case of water repellent leaves, airborne dust particles can be removed by water droplets that roll off the (self-cleaning) surfaces [1]. The leaves of *N. nucifera* afford an impressive

demonstration of this effect, which is, therefore, called the "Lotus-Effect" [1].

This remarkable ability of nature has inspired numerous researchers to fabricate surfaces which imitate the surface structures of the superhydrophobic biosurfaces, by using numerous techniques and methods, for example, plasma treatment [8–10], photolithography [11, 12], casting polymers under controlled conditions or on appropriately designed/selected templates[13–17], sol-gel [18–21], electrospinning [22], deposition of nanoparticles on smooth or microroughened substrates [23–28], deposition of nanoparticle-polymer composites on smooth surfaces [29–32], growth of aligned nanotube [33, 34] or polyacrylonitrile nanofibers [35], laser fabrication [36–38], and controlled grain growth [39]. In most of the aforementioned studies the generated textured topographies are composed of inherent hydrophilic materials (Young contact angle, $\theta_Y < 90°$) and therefore their surfaces are chemically treated to induce hydrophobicity. Because of the two-length-scale hierarchical structure and the hydrophobic character of the surface, enhanced water repellency (superhydrophobicity) is achieved. It is noteworthy, however, that in some studies superhydrophobicity was induced on inherent hydrophilic materials, without any chemical modification of their surfaces [32, 39]. These studies offered support to Hermingshaus's model, which predicts that only the material hierarchical structure determines its wettability [2].

Water repellent coatings can be important in many applications including for example the prevention of icing in cold weather and the promotion of self-cleaning processes induced by rainwater on outdoor surfaces (automobiles, buildings, antennas, traffic lights, etc.), the prevention of clotting in artificial blood vessels, the decrease of corona activity developed in conductors of transmission lines under rainy conditions, the production of waterproof and stain resistant textiles and the reduction of friction in water (boat or swimsuit coatings) [9, 36, 40, 41]. Another promising application of the superhydrophobic coatings is their use as surface protective barriers for the preservation and conservation of monuments. The most important degradation factor of outdoor, immovable cultural heritage is rainwater which can cause stone deterioration through cycles of freezing and thawing inside the pores of the stone or by intraporous crystallization of the salts transferred by water. For this reason, the application of hydrophobic coatings has been suggested as a potential strategy for the surface protection of outdoor cultural heritage assets [42–49]. We have recently described a very simple method that can be used to impart superhydrophobicity to a large variety of different surfaces including marble, a material that has been very often used in cultural heritage objects [32, 50]. The method is summarized as follows [32]: nanoparticles are dispersed in a (siloxane or acrylic) polymer solution. The mixture is then sprayed on the substrate and the resulting composite polymer-nanoparticle film exhibits superhydrophobic properties.

In the present study the aforementioned method is employed to treat Opuka marlstone, Božanovský sandstone and Hořický sandstone, which have been used for the restoration of the castle of Prague. Two commercially available poly (alkyl siloxanes) "Rhodorsil 224" and "Porosil VV plus" are used to treat the surfaces of the stones. The two siloxanes are used by conservators as surface protective coatings for monuments; Porosil has been actually used in the conservation of the castle of Prague. The first goal of the study is to demonstrate that the hydrophobic character of the siloxanes, used by conservators, can be easily enhanced by mixing them with nanoparticles. The siloxane-nanoparticle composites are sprayed on the stones and the treated surfaces exhibit superhydrophobic properties. It is shown that superhydrophobicity can be achieved (i) on any of the three stones used in the restoration of the castle of Prague and using (ii) both Rhodorsil and Porosil and (iii) various, common nanoparticles such as silica (SiO_2), alumina (Al_2O_3), tin oxide (SnO_2) and titanium oxide (TiO_2). Consequently, superhydrophobicity is induced on various stone surfaces by a one step, low-cost and very simple method, which can be applied to treat large surfaces (monuments) by conservators and restorators, as it does not include the use of any sophisticated instrumentation and/or expensive materials. Superhydrophobicity is attributed to the textured surfaces of the siloxane-particle composite films. Water repellency, evaluated by contact angle measurements, cannot be the only criterion for the selection of a product used for the protection of outdoor cultural heritage. A good protective material must not affect the aesthetic appearance of the stone substrate, should assure a good permeability for water vapor and must decrease the amount of water absorbed by capillarity. The investigation of the effect of the nanoparticles in the properties of Rhodorsil and Porosil with respect to the aforementioned criteria is the second goal of the study.

2 Experimental

Three stones, described in Table 1 and used for the restoration of the castle of Prague, were included in the study. Stone specimens were squared blocks of around 2.5 × 2.5 × 1 cm and were obtained from local suppliers in Prague. Specimens were washed with deionized water and acetone and dried. The chemical compositions of the stones were found in the literature [51, 52] and were confirmed by X-ray diffraction (XRD) analysis, which was performed using a Rich.Seifert 3003 TT diffractometer with Ni-filtered Cu Kα radiation ($\lambda = 0.154$ nm). The 2θ scanning range was varied from 5° to 80° with a step of 0.01° and a measuring time of 15 s per step. Open porosity and specific gravity were

Table 1 Stones included in the study. Compositions were found in the literature [51, 52] and some data were confirmed by XRD. Open porosity, specific gravity and colorimetric measurements were carried out according to the Experimental section

Stone	Composition	Open porosity (%)	Specific gravity (g/cm^3)	Colorimetric measurements		
				L^*	a^*	b^*
Opuka	40–70% SiO_2, 10–30% $CaCO_3$, 10–20% feldspars, other	7.7	2.23	77.7	4.0	15.8
Božanovský	71–80% SiO_2, 5–8% feldspars, 3–5% rock fragments, 3–4% mica, grains of heavy minerals	7.0	2.19	72.3	4.3	11.8
Hořický	69% SiO_2, 1% feldspars, 26% clay minerals, 3% limonite, 1% heavy minerals	11.3	1.95	69.0	4.4	18.4

measured by weighing the saturated surface dry mass of the substrates according to the RILEM Technical Recommendations [53]. Stone specimens were then treated according to the following procedures.

Two commercially available poly (alkyl siloxane) products in white spirit, Rhodorsil 224 (Rhodia Silicones) 7% wt and Porosil VV plus (AquaBarta) 10% wt, were used as received. Silica (SiO_2) particles (fumed powder, Aldrich) with a 7 nm mean diameter were dispersed (2.0% w/v) in the siloxane solutions. Dispersions were subsequently stirred vigorously for 20 min. The siloxane–SiO_2 dispersions were immediately sprayed onto the stone substrates of Table 1 for 2 s through a nozzle with a diameter of 733 μm using an airbrush system (Paasche Airbrush). For comparison, pure siloxane solutions (no particles) were also sprayed onto the stone substrates. Coated samples were annealed at 40° overnight in vacuum to remove residual solvent and kept at room temperature for 2 to 3 days.

Contact angle measurements were carried out on the stones, coated with pure siloxanes and siloxane–SiO_2 composite films, by the sessile drop method using a Krüss DSA 100 (Krüss) apparatus and distilled water. Water droplets (2–4 μL) were delivered to different points of each specimen and from a height sufficiently close to the substrate so that the needle remained in contact with the liquid droplet. Then, the delivery needle was withdrawn with minimal perturbation to the drop [54] and the image of the drop was captured immediately for static contact angle measurement. The contact angle hysteresis was calculated by the dynamic sessile drop method. The advancing/receding contact angle was the maximum/minimum angle measured whereas the volume of the droplet was increased/decreased without increasing/decreasing the solid-liquid interfacial area. The reported contact angle values are averages of five measurements; variations are mentioned in the text or are shown in the plots as error bars.

Water vapor permeability, water absorption by capillarity and colorimetric measurements were performed on the stones, treated with pure siloxanes and siloxane–SiO_2 composite films, and compared with corresponding measurements carried out on untreated, bare stone substrates, according to the following procedures. For the vapor permeability tests, sample blocks were fixed on top of cylindrical PVC containers that were partially (1/2) filled with water. Then, the sealed containers were placed in a climatic chamber, kept at R.H. 25% and $T = 40 \pm 0.5$°C. The containers were weighted every 24 h. It was assumed that the vapor flow through the stone had reached a constant value when the difference between two consecutive daily (24 h) weight variations, ΔM_{i-1} and ΔM_i, was less than 5%:

$$\frac{\Delta M_i - \Delta M_{i-1}}{\Delta M_i} \times 100 < 5\% \quad (1)$$

Under constant vapor flow the water vapor permeability was evaluated as the mass of water vapor passing though the surface unit (cm^2) in 24 h. Three consecutive measurements with intervals of 24 h were carried out. Average values are reported and deviations are provided as error bars. Capillary water absorption measurements were performed by the gravimetric sorption technique. The dried weighted sample blocks were placed (with the treated sides) on a filter paper pad (1 cm of Whatman paper, No. 4) partially immersed in distilled water. After 1 h the samples were removed and weighted again to determine the amounts of water absorbed by capillary forces. The results are averages of three measurements. Colorimetric measurements were taken on three homogeneous spot areas of 4 mm in diameter using

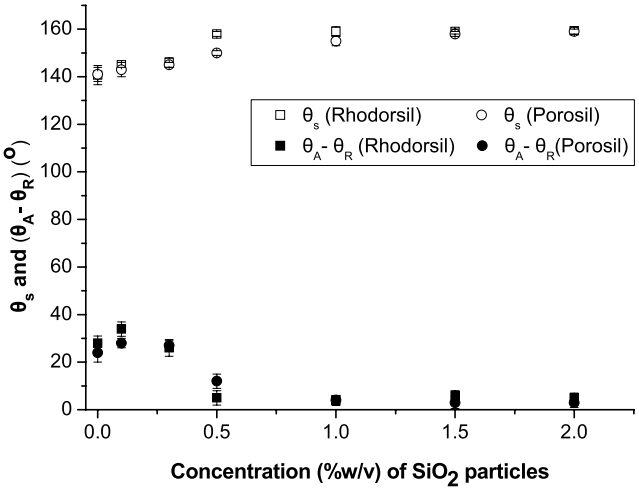

Fig. 1 Static contact angle (θ_S) and contact angle hysteresis ($\theta_A - \theta_R$) of Rhodorsil–SiO_2 and Porosil–SiO_2 films deposited on Opuka vs. the concentration of SiO_2 particles

a portable reflectance spectrophotometer MiniScan XE Plus (HunterLab Associates Inc.). The results were evaluated by the use of $L^*a^*b^*$ coordinates of the CIE 1976 scale.

More samples were prepared for contact angle measurements using the spraying technique described previously. Rhodorsil–SiO_2 and Porosil–SiO_2 dispersions with particle concentrations of 0.1, 0.3, 0.5, 1.0, 1.5, and 2.0% w/v were deposited on Opuka specimens. Titanium oxide (TiO_2), tin oxide (SnO_2) and alumina (Al_2O_3) nanoparticles were dispersed in Rhodorsil and Porosil solutions at a concentration of 10% w/v and were then deposited on Opuka samples. According to the manufacturer (Alfa Aesar), particle dimensions were 5, 22–43 and 40–50 nm for TiO_2, SnO_2 and Al_2O_3 respectively. Finally, Rhodorsil and Porosil solutions were spin coated onto clean glass surfaces to produce smooth surfaces, which were used to measure the Young contact angles (θ_Y).

The morphologies of the treated surfaces, prepared in this study, were investigated by scanning electron microscopy (SEM, Jeol-JSM 840A) and by atomic force microscopy, operated in tapping mode (AFM, Multimode IIId, Veeco Inc.)

3 Results and discussion

Preliminary XRD experiments were performed to collect some data regarding the qualitative compositions of the stones, which were then confirmed by detailed, quantitative compositions found in the literature [51, 52]. In particular, SiO_2, was detected in all three stones of Table 1 and $CaCO_3$, was found in Opuka. Stone compositions are summarized in Table 1. The latter includes porosity and colorimetric measurements, performed on bare, untreated stones. These data are used for later discussion.

Figure 1 shows water static contact angle (θ_S) and contact angle hysteresis measurements, defined as the difference of the advancing (θ_A) and receding contact angle (θ_R), as a function of particle concentration for Rhodorsil–SiO_2 and Porosil–SiO_2 composite films deposited on Opuka stone. No major difference is observed in the measurements collected for the two polymers, as these are of similar nature; both are poly (alkyl siloxanes). This is evidenced by θ_S measurements performed on spin coated films on glass surfaces. As the films applied by spin coating are very/atomically smooth any effect on the contact angle originating from surface roughness (Wenzel or Cassie–Baxter models [55, 56]) is suppressed and therefore the measured θ_S is very close to the Young contact angle which is of course an intrinsic property of the material. It is reported that the (Young) contact angles of smooth Rhodorsil and Porosil films were comparable as they were found to be $102 \pm 1°$ and $104 \pm 1°$, respectively. Figure 1 shows that θ_S increases initially with particle concentration and reaches a maximum value (159° for both Rhodorsil–SiO_2 and Porosil–SiO_2 films) when the particle concentration in the dispersion is >0.5% w/v. Further increase in particle concentration does not have any effect on θ_S. The contact angle hysteresis first increases with particle concentration, then decreases and finally becomes constant and very small (5° and 3° for Rhodorsil–SiO_2 and Porosil–SiO_2 films, respectively). It is noteworthy that the variations of θ_S and $\theta_A - \theta_R$ with particle concentration (Fig. 1) are in agreement with previously published results which were collected for Rhodorsil–SiO_2 and PMMA–SiO_2 films, deposited on glass surfaces [32]. In the previous report a detailed discussion is provided to explain the variation of θ_S and $\theta_A - \theta_R$ with particle concentration, based on the film morphologies which were elucidated by SEM; a brief summary of this discussion is provided later. We note, however, that in the present study our goal of is to impart superhydrophobicity to stone materials and therefore we focus on the siloxane-particle composite films which were prepared from dispersions of high particle concentration (>0.5% w/v).

The high and low values of θ_S and $\theta_A - \theta_R$, respectively, measured for films prepared from dispersions with elevated particle concentration (>0.5% w/v) suggest that the surfaces of these siloxane-particle composite films exhibit enhanced water repellency. This is supported by Fig. 2, which shows that a drop bounces off when it impacts an Opuka surface treated with a Rhodorsil-particle composite film. The latter was prepared from a dispersion with 1.5% w/v particle concentration. Finally, the drop rolls off the treated substrate and does not stick on the surface, which preserves its dryness.

Superhydrophobicity was induced on the surfaces of the other two stones included in this study. Table 2 shows the results of θ_S and $\theta_A - \theta_R$ measurements, performed on surfaces of Božanovský and Hořický stones, which were

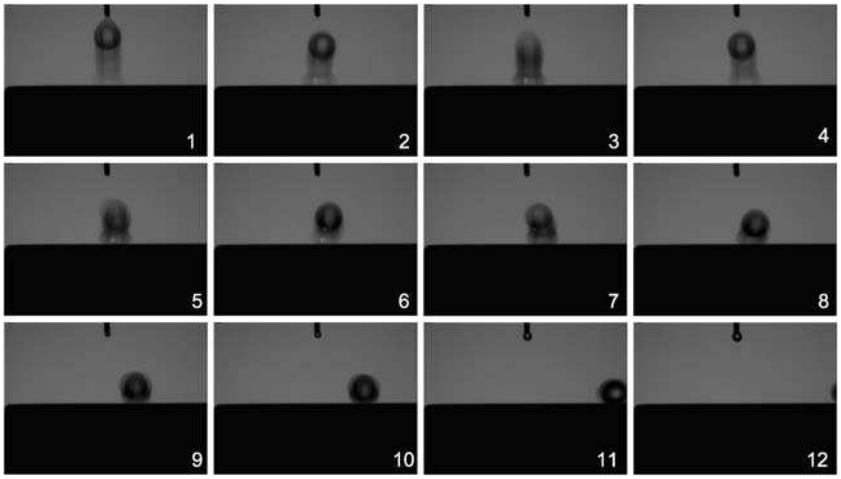

Fig. 2 Water droplet bouncing on Opuka which was treated with Rhodorsil solution mixed with 1.5% w/v SiO_2 nanoparticles. A sequence number is provided in the *lower right* corner of each photograph

Table 2 Static contact angle (θ_S) and contact angle hysteresis ($\theta_A - \theta_R$) measured on stone surfaces, which were treated with pure Rhodorsil, Rhodorsil–SiO_2, pure Porosil and Porosil–SiO_2. Siloxane-particle composite films were prepared from dispersions with particle concentration 2% w/v

Contact angle	Particle concentration (w/v)	Rhodorsil			Porosil		
		Opuka*	Božanovský	Hořický	Opuka*	Božanovský	Hořický
θ_S (°)	0	141 ± 4	134 ± 3.5	140 ± 1.5	141 ± 3	140 ± 4	143 ± 2
	2%	159 ± 1.5	157 ± 2	155 ± 3	159 ± 1	158 ± 2.5	156 ± 2
$\theta_A - \theta_R$ (°)	0	28 ± 3	38 ± 4	38 ± 3	24 ± 4	35 ± 4	33 ± 5
	2%	5 ± 2	5 ± 2	6 ± 2	3 ± 2	5 ± 2	5 ± 2

*Reproduced from Fig. 1

treated with pure siloxanes (Rhodorsil and Porosil) and siloxane-particle (2% w/v) composite films. For comparison, measurements on treated Opuka, discussed previously, are also included. The following conclusions can be drawn from the results of Table 2: (i) superhydrophobicity was achieved on both Rhodorsil–SiO_2 and Porosil–SiO_2 films applied on any of the three substrates i.e. high θ_S (>150°) and low $\theta_A - \theta_R$ (<7°) were measured on the surface of any composite-substrate combination. As it was expected, the surfaces of pure siloxanes (no particles) applied on the stone substrates were hydrophobic with, however, substantially lower θ_S (<145°) and higher $\theta_A - \theta_R$ (>20°), compared to the siloxane-particle composite films. Consequently, superhydrophobicity was induced by the SiO_2 nanoparticles. (ii) Static contact angles measured for the siloxane-particle composite films were found to be nearly independent of the substrate material. When Rhodorsil was used for the application of the composite films, the mean values of θ_S varied by ±2° (155–159°). In the case of Porosil, the corresponding variation of the mean θ_S was only ±1.5° (156–159°). Similarly, small variations are reported in Table 2 for the $\theta_A - \theta_R$ measurements, suggesting thus that the underlying substrate has negligible effect on the wettability of the deposited siloxane-particle composite films. It is noteworthy that the same conclusion was reported in a previous report in which polymer-particle composite films were applied on a large variety of substrates including glass, silicon, concrete, aluminum, silk, wood and marble [32]. (iii) The type of the siloxane (Rhodorsil or Porosil) did not have any major effect on the measured θ_S and $\theta_A - \theta_R$. This is valid for either pure siloxanes or siloxane-particle composite films. The same was observed in Fig. 1 and was attributed to the similar nature of the two siloxanes used in this study.

The origin of the observed superhydrophobicity on the surfaces of the siloxane-particle films is elucidated in Fig. 3. Figure 3a shows the surface of the bare, untreated Božanovský stone. When pure siloxane is deposited on the stone surface, a continuous film is formed which follows the roughness of the underlying substrate (Fig. 3b). Apparently this surface is not superhydrophobic according to the θ_S and $\theta_A - \theta_R$ values reported in Table 2. When the Božanovský stone is treated with a siloxane–SiO_2 dispersion of high particle concentration (2% w/v), protruded particle aggregates are formed on the surface according to Fig. 3c. We note that a similar morphology (i.e. protruded aggregates) was observed on glass surfaces treated with polymer-nanoparticle dispersions, as it was described in a previous report [32]. Aggregates are separated by small, relatively "smooth" ar-

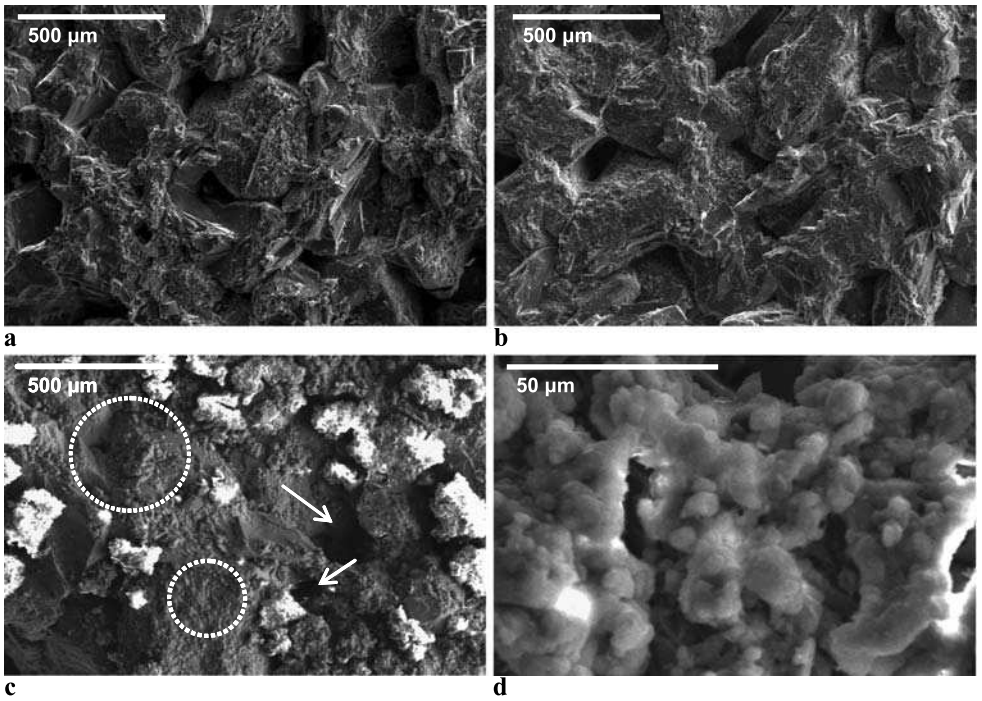

Fig. 3 SEM images of Božanovský stone (**a**) untreated, (**b**) treated with pure Porosil and (**c**) and (**d**) treated with Porosil-2% w/v SiO_2. The hierarchical (**c**) micrometer- and (**d**) nanometer-sized structures are shown. Protruded aggregates formed at the micrometer scale are separated by "smooth" areas; some of them are indicatively shown by *circles* in (**c**). *Arrows* are included in (**c**) to show large pores for later discussion

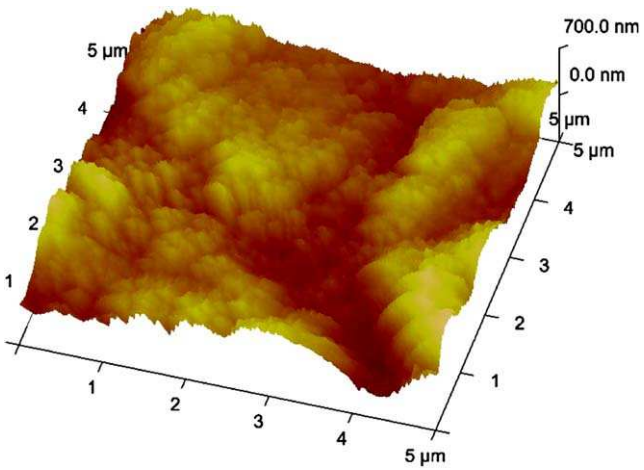

Fig. 4 AFM image collected on the surface of a protruded aggregate which was formed after the deposition of Rhodorsil-2% w/v SiO_2. Nanometer-sized structures are shown (as in Fig. 3d)

eas, which resemble the film produced by the deposition of pure siloxane with no particles (some of these areas are shown in Fig. 3c by circles). Figure 3d shows that the randomly distributed aggregates consist of further nanostructures implying that a two-length-scale hierarchical structure is formed on the surface, which is responsible for the observed superhydrophobicity [8–39]. Figure 4, shows an AFM image collected on the surface of a protruded aggregate formed on Rhodorsil–SiO_2 film and provides further evidence on the nanoscale roughness, shown also in Fig. 3d for Porosil–SiO_2 film.

Superhydrophobicity was not achieved when stone surfaces were treated with dispersions which corresponded to low particle concentrations (e.g. $<1\%$ w/v according to Fig. 1). As was mentioned, the morphologies of these surfaces were studied previously in detail and were used to elucidate contact angle measurements which followed the trend of the data reported in Fig. 1 [32]. In the present study these surfaces are not of any interest and therefore they are just briefly discussed next. Figure 1 shows that low θ_S and large $\theta_A - \theta_R$ were recorded on films prepared from dilute particle dispersions, indicating that the Cassie–Baxter scenario (superhydrophobic state) which suggests that a water droplet sits on a mixture of air and solid is not realistic for the surfaces of these films. Particle aggregates were formed in these films but they were separated by "smooth" areas which were much larger than those shown in Fig. 3c (which corresponds to particle concentration of 2% w/v). The elevated hysteresis reported for films prepared from dispersions of low particle concentration can be explained if we consider that water may fill the large, smooth areas that exist among the aggregates. On the other hand, water does not fill the small smooth crevices formed when dispersions of high particle concentrations are used for treatment (Fig. 3c) and therefore in this case the Cassie–Baxter scenario appears to be realistic. The variation of $\theta_A - \theta_R$ in Fig. 1 is not surprising, as it is in agreement with previous studies. The surface roughness of the composite films increases with particle concentration thus leading to the conclusion that the x-axis of Fig. 1 corresponds qualitatively to surface roughness [32]. Based on that, we note that a very good agreement exists between the

variation of $\theta_A - \theta_R$ shown in Fig. 1 and the results reported for roughened wax [57, 58] plasma-treated PDMS [10], and Teflon [59] surfaces. In all of these studies, hysteresis first increases with roughness, then decreases rapidly, and finally becomes constant (similar to Fig. 1).

So far it was demonstrated that superhydrophobicity can be achieved on the surfaces of the three stones of Table 1 using commercial siloxane products mixed with SiO_2 nanoparticles. Table 3 shows that the type or size of the nanoparticles used to impart superhydrophobicity does not affect the wettability of the siloxane-nanoparticle film surface. High (>150°) and comparable values of θ_S were measured on Opuka samples treated with Rhodorsil and Porosil solutions which were mixed with Al_2O_3, SnO_2 and TiO_2 nanoparticles. It is important to note, however, that as it was shown in Fig. 1, a key parameter to achieving superhydrophobicity is the particle concentration. For Rhodorsil/Porosil–SiO_2 composites, it was found that superhydrophobicity is achieved when the particle concentration is >0.5% w/v (Fig. 1). Preliminary experiments were performed using the nanoparticles of Table 3 to assess the particle concentration, above which θ_S exhibits saturation behavior. It was found that elevated particle concentrations are necessary to obtain high and constant θ_S. The contact angles in Table 3 correspond to particle concentrations of 10% w/v; further increase (or slight decrease) in particle concentration did not have any effect on the reported values.

In addition to water repellence, a good stone protective material should assure a good permeability for water vapor which is quantified by the % reduction of vapor permeability (RVP%) according to (2):

$$\mathrm{RVP\%} = \left(\frac{m_{uv} - m_{tv}}{m_{uv}}\right) \times 100 \qquad (2)$$

where m_{uv} and m_{tv} are the masses of water vapor penetrating the untreated and the treated substrate, respectively. Apparently, an ideal coating must have no effect on the water vapor permeability (RVP = 0). Results of RVP% measurements are shown in Fig. 5a for Rhodorsil based coatings and Fig. 5b for Porosil based coatings (with and without SiO_2 particles), applied on the three stones of Table 1. Measurements reported previously for Pentelic marble treated with Rhodorsil based coatings are included in Fig. 5a to show that the vapor permeability of this stone decreases drastically when nanoparticles are used for surface treatment along of course with siloxane (in this case Rhodorsil) [50]. On the contrary nanoparticles do not have any significant effect on the RVP% measurements performed on treated Opuka, Božanovský and Hořický stones. The value of RVP% recorded for each stone treated with pure silox-

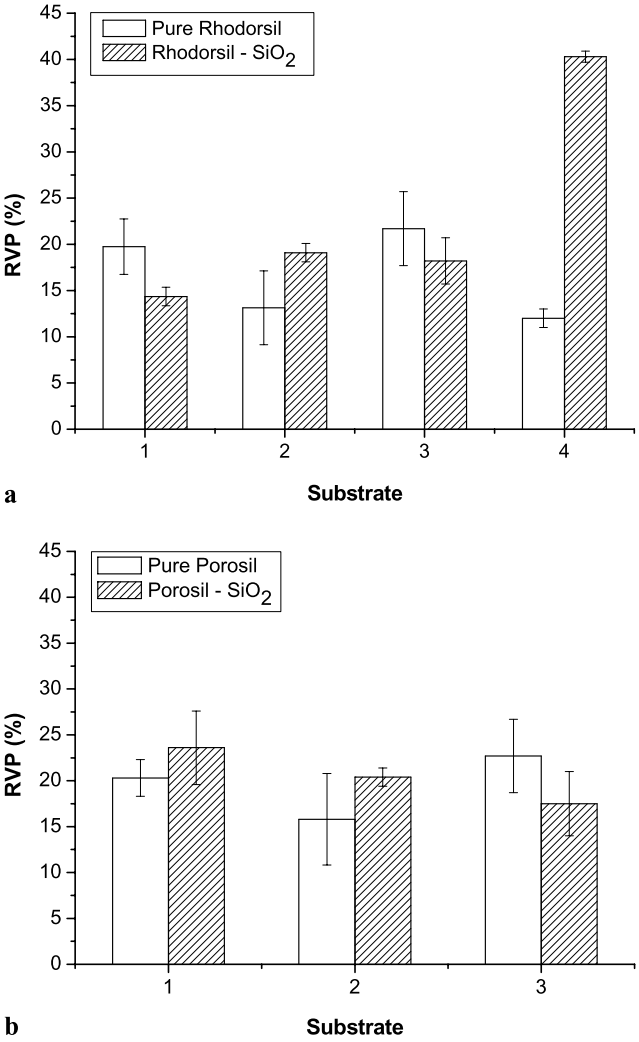

Fig. 5 Reduction of vapor permeability % (RVP%) measured on Opuka (1), Božanovský (2) and Hořický (3) stones, which were treated with (**a**) pure Rhodorsil and Rhodorsil–SiO_2 and (**b**) pure Porosil and Porosil–SiO_2. For comparison, measurements reported previously [50] for Pentelic marble treated with pure Rhodorsil and Rhodorsil–SiO_2 are included in (**a**). All siloxane-particle composite films were prepared from dispersions with particle concentration 2% w/v

Table 3 Static contact angle (θ_S) measured on Opuka surfaces, which were treated with Rhodorsil and Porosil solutions mixed with various nanoparticles: Al_2O_3 (40–50 nm), SnO_2 (22–43 nm) and TiO_2 (5 nm)

Contact angle	Particle concentration (w/v)	Rhodorsil			Porosil		
		Al_2O_3	SnO_2	TiO_2	Al_2O_3	SnO_2	TiO_2
θ_S (°)	10%	162 ± 2	159 ± 2	158 ± 3	157 ± 1	158 ± 1	155 ± 3

Table 4 Measurements of % reduction of water absorption by capillarity performed on stone surfaces, treated with pure Rhodorsil, Rhodorsil–SiO_2, pure Porosil and Porosil–SiO_2. Siloxane-particle composite films were prepared from dispersions with particle concentration 2% w/v

Particle concentration (w/v)	Rhodorsil			Porosil		
	Opuka	Božanovský	Hořický	Opuka	Božanovský	Hořický
0	88.5 ± 2	96.5 ± 0.5	97.7 ± 0.5	94 ±2	97.2 ± 0.7	98.1 ± 0.1
2%	94 ±0.8	97.6 ± 0.7	98.1 ± 0.2	94.5 ± 1.5	97.6 ± 0.9	98.3 ± 0.2

ane is comparable with the corresponding RVP% measurement performed on the same stone covered by a siloxane-particle composite film. Some deviations between stones treated with pure siloxane and composite films are observed but these do not follow a particular trend and furthermore are within the error bars (except probably for the results which correspond to Opuka in Fig. 5a). In summary, Fig. 5 suggests that the water vapor permeability through the treated stones of Table 1 is not affected by the nanoparticles, in contrast to treated marble in which nanoparticles impede vapor flow [50]. We speculate that this contrast is based on the large porosity difference between Pentelic marble (0.21% [50]) and the three stones of Table 1 (7–11.3%). In the case of low porosity stones (marble) particle aggregates formed on the surface after treatment with a siloxane-nanoparticle dispersion, may inhibit vapor flow. However, the augmented porosity of Opuka, Božanovský and Hořický stones assures a good permeability for vapor. This is illustrated in Fig. 3c: large pores, shown by arrows, exist on the surface of Božanovský stone, treated with Porosil–SiO_2. Water vapor can easily flow through these pores.

The evaluation of the efficacy of a coating to protect monument surfaces and cultural heritage materials should include measurements of capillary water absorption [42, 43, 45–48]. Water contact angle measurements are not adequate, as water can invade the stone also by capillary absorption. The methodology is described in the Experimental section and the results of this investigation are summarized in Table 4. The % reduction of water absorption by capillarity (RC%) is defined in (3):

$$\mathrm{RC\%} = \left(\frac{m_{uw} - m_{tw}}{m_{uw}}\right) \times 100 \tag{3}$$

where m_{uw} and m_{tw} are the masses of water absorbed by capillarity by the untreated (bare) and treated substrate, respectively. Apparently, an ideal coating must eliminate the amount of water absorbed by capillarity (RC% = 100). Table 4 shows that a considerable reduction in the quantity of the absorbed water was achieved when siloxane–SiO_2 composite films were applied on the stone surfaces (94–98.3%), which however is comparable to the corresponding reduction measured for stones treated with pure siloxanes (88.5–98.1%). Therefore the same conclusion as drawn previously for the RVP% measurements is reported here as well: RC% is not affected significantly by the nanoparticles. We cannot envision any obvious reason for this result, apart from the augmented porosity of the stones included in this study, as it was discussed previously.

An ideal protective film should have no effect on the aesthetic appearance of the treated stone. Colorimetric measurements were performed to evaluate the global color differences (ΔE^*) of the stone surfaces, due to treatment, according to (4):

$$\Delta E^* = \sqrt{\Delta L^{*2} + \Delta a^{*2} + \Delta b^{*2}} \tag{4}$$

where L^*, a^* and b^* are the brightness (0 for black—100 for white), the red–green component (positive for red and negative for green) and the yellow–blue component (positive for yellow and negative for blue), respectively. Results of ΔE^* measurements are shown in Fig. 6a for Rhodorsil based coatings and Fig. 6b for Porosil based coatings (with and without SiO_2 particles), applied on the three stones of Table 1. Overall, Fig. 6 shows that ΔE^* increases when SiO_2 nanoparticles are used in the protective film i.e. ΔE^* measured for stones treated with siloxane–SiO_2 films are clearly higher than the ΔE^* recorded for stones treated with pure siloxanes (no particles). We note that the color change (ΔE^*) caused by the pure siloxane films was mainly due to the contribution of the L^* component (brightness), which decreased when stones were covered by the siloxanes. The high values of ΔE^* reported for the stones treated with siloxane–SiO_2 films were originated mainly by the contribution of the b^* component, which decreased drastically, when white SiO_2 (L^* : 88, a : −2.5, b^* : −7) particles were added in the protective film, resulting thus in an elevated Δb^*. The nanoparticles also affected somewhat the brightness (L^*) of the stones. Figure 6 shows that the effect of the SiO_2 nanoparticles in the color change of the Hořický stone was more pronounced compared to the other two stones. This is because the values of the L^* and b^* components measured for this stone differ a lot, and more than the L^* and b^* of the other two stones, from the corresponding L^* and b^* of the SiO_2 particles. This is easily shown if the L^* and b^* values reported in Table 1 for the three stones are compared with the $L^* = 88$ and $b^* = -7$ of the SiO_2 particles.

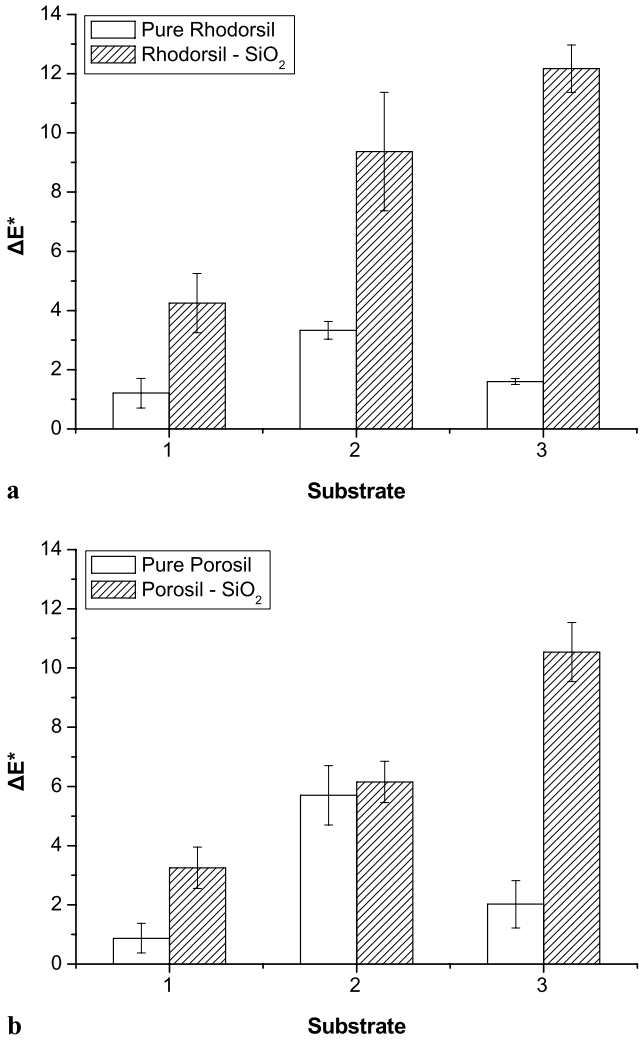

Fig. 6 Total color difference (ΔE^*) of Opuka (1), Božanovský (2) and Hořický (3) stones, treated with (**a**) pure Rhodorsil and Rhodorsil–SiO_2 and (**b**) pure Porosil and Porosil–SiO_2. Siloxane-particle composite films were prepared from dispersions with particle concentration 2% w/v

4 Conclusions

We have presented a very simple method that can be used to impart superhydrophobicity to stone surfaces of monuments using common and low-cost materials that are already employed or are easy to be found by conservators. Siloxane-nanoparticle dispersions were sprayed on stones, and this process resulted in the formation of rough two-length-scale hierarchical structures that exhibited water repellent properties. It was shown that superhydrophobicity can be achieved, by this simple method (i) on the surfaces of three types of stones, Opuka, Božanovský and Hořický, which have been used for the restoration of the castle of Prague, (ii) using two siloxane products such as Rhodorsil 224 and Porosil VV plus, which are utilized by conservators and (iii) using common nanoparticles such as silica (SiO_2), alumina (Al_2O_3), tin oxide (SnO_2) and titanium oxide (TiO_2). The effect of the particle concentration on the wettability of the siloxane-particle surfaces was briefly investigated for siloxane–SiO_2 composites deposited on Opuka. It was found that superhydrophobicity was achieved only when the stone is treated with dispersions of high (>0.5% w/v) particle concentration. It was shown that the stone substrate and the nanoparticle size (5–50 nm) or type have almost no effect on the wettability of the surfaces of the siloxane-particle films, as comparable contact angles were measured on the three stone substrates, treated with any siloxane-particle composite.

Nanoparticles induced superhydrophobicity but they did not have any obvious effect on the results of the capillary water absorption and the water vapor permeability tests. Treatment of the stones with pure (hydrophobic) siloxanes and siloxane–SiO_2 (superhydrophobic) composites resulted in comparable reductions of the water vapor permeability and the water amounts absorbed by capillarity. However, the aesthetic appearance of the three stones, included in this study was highly affected by the nanoparticles. Colorimetric measurements showed that ΔE^* measured after treating the stones with siloxane-particle films was clearly higher than the color change recorded when pure siloxanes were applied on the surfaces of the stones.

Acknowledgements We thank L. Papadopoulou, M. Stefanidou and S. Marras for their help in SEM, porosity measurements and XRD measurements, respectively. Support by the Greek Ministry of Development (GSRT) and the European Social Fund (EU) through the research program PENED2003 is gratefully acknowledged. Financial support to P.N. Manoudis by the Greek State Scholarship Foundation is also gratefully acknowledged.

References

1. W. Barthlott, C. Neinhuis, Planta **202**, 1 (1997)
2. S. Herminghaus, Europhys. Lett. **52**, 165 (2000)
3. P. Wagner, R. Fürstner, W. Barthlott, C. Neinhuis, J. Exp. Bot. **54**, 1295 (2003)
4. T. Sun, L. Feng, X. Gao, L. Jiang, Acc. Chem. Res. **38**, 644 (2005)
5. T. Wagner, C. Neinhuis, W. Barthlott, Acta Zool. (Stockholm) **77**, 213 (1996)
6. G.S. Watson, J.A. Watson, Appl. Surf. Sci. **235**, 139 (2004)
7. W. Lee, M.K. Jin, W.C. Yoo, J.K. Lee, Langmuir **20**, 7665 (2004)
8. W. Chen, A.Y. Fadeev, M.C. Hsieh, D. Öner, J. Youngblood, T.J. McCarthy, Langmuir **15**, 3395 (1999)
9. S.R. Coulson, I. Woodward, J.P.S. Badyal, S.A. Brewer, C.J. Willis, J. Phys. Chem. B **104**, 8836 (2000)
10. A.D. Tserepi, M.-E. Vlachopoulou, E. Gogolides, Nanotechnology **17**, 3977 (2006)
11. D. Öner, T.J. McCarthy, Langmuir **16**, 7777 (2000)
12. L. Gao, T.J. McCarthy, Langmuir **22**, 2966 (2006)
13. H.Y. Erbil, A.L. Demirel, Y. Avci, O. Mert, Science **299**, 1377 (2003)
14. H. Yabu, M. Takebayashi, M. Tanaka, M. Shimomura, Langmuir **21**, 3235 (2005)
15. M. Sun, C. Luo, L. Xu, H. Ji, Q. Ouyang, D. Yu, Y. Chen, Langmuir **21**, 8978 (2005)

16. R. Fürstner, W. Barthlott, C. Neinhuis, P. Walzel, Langmuir **21**, 956 (2005)
17. L. Zhang, Z. Zhou, B. Cheng, J.M. DeSimone, E.T. Samulski, Langmuir **22**, 8576 (2006)
18. N.J. Shirtcliffe, G. McHale, M.I. Newton, C.C. Perry, Langmuir **19**, 5626 (2003)
19. B. Mahltig, H. Böttcher, J. Sol-Gel Sci. Technol. **27**, 43 (2003)
20. M. Hikita, K. Tanaka, T. Nakamura, T. Kajiyama, A. Takahara, Langmuir **21**, 7299 (2005)
21. L. Gao, T.J. McCarthy, J. Am. Chem. Soc. **128**, 9052 (2006)
22. M. Ma, R.M. Hill, J.L. Lowery, S.V. Fridrikh, G.C. Rutledge, Langmuir **21**, 5549 (2005)
23. L. Zhai, C.F. Cebeci, R.E. Cohen, M.F. Rubner, Nano Lett. **4**, 1349 (2004)
24. T. Soeno, K. Inokuchi, S. Shiratori, Appl. Surf. Sci. **237**, 543 (2004)
25. D. Lee, M.F. Rubner, R.E. Cohen, Nano Lett. **6**, 2305 (2006)
26. J. Bravo, L. Zhai, Z. Wu, R.E. Cohen, M.F. Rubner, Langmuir **23**, 7293 (2007)
27. H.-M. Bok, T.-Y. Shin, S. Park, Chem. Mater. **20**, 2247 (2008)
28. M. Motornov, R. Sheparovych, R. Lupitskyy, E. MacWilliams, S. Minko, Adv. Mater. **20**, 200 (2008)
29. C.-T. Hsieh, J.-M. Chen, R.-R. Kuo, T.-S. Lin, C.-F. Wu, Appl. Surf. Sci. **240**, 318 (2005)
30. E. Chibowski, L. Hołysz, K. Terpilowski, M. Jurak, Colloids Surf. A **291**, 181 (2006)
31. M.Y. Yüce, A.L. Demirel, F. Menzel, Langmuir **21**, 5073 (2005)
32. P.N. Manoudis, I. Karapanagiotis, A. Tsakalof, I. Zuburtikudis, C. Panayiotou, Langmuir **24**, 11225 (2008)
33. S. Li, H. Li, X. Wang, Y. Song, Y. Liu, L. Jiang, D. Zhu, J. Phys. Chem. B **106**, 9274 (2002)
34. K.K.S. Lau, J. Bico, K.B.K. Teo, M. Chhowalla, G.A.J. Amaratunga, W.I. Milne, G.H. McKinley, K.K. Gleason, Nano Lett. **3**, 1701 (2003)
35. L. Feng, S. Li, Y. Li, L. Zhang, J. Zhai, Y. Song, B. Liu, L. Zhiang, D. Zhu, Adv. Mater. **14**, 1857 (2002)
36. V. Zorba, E. Stratakis, M. Barberoglou, E. Spanakis, P. Tzanetakis, S.H. Anastasiadis, C. Fotakis, Adv. Mater. **20**, 4049 (2008)
37. V. Zorba, E. Stratakis, M. Barberoglou, E. Spanakis, P. Tzanetakis, C. Fotakis, Appl. Phys. A **93**, 819 (2008)
38. M. Zhou, H.F. Yang, B.J. Li, J. Dai, J.K. Di, E.L. Zhao, L. Cai, Appl. Phys. A (2008). doi:10.1007/s00339-008-4920-5
39. W. Xiao, Z. Huang, Z. He, Appl. Phys. Lett. **89**, 083101 (2006)
40. A. Nakajima, K. Hashimoto, T. Watanabe, Monatsh. Chem. **132**, 31 (2001)
41. M. Callies, D. Quéré, Soft Matter **1**, 55 (2005)
42. L. Appolonia, V. Fassina, U. Matteoli, A.M. Mecchi, M.P. Nugari, D. Pinna, R. Peruzzi, O. Salvadori, U. Santamaria, A. Scala, P. Tiano, in *Proceedings of International Colloquium on Methods of Evaluating Products for the Conservation of Porous Building Material in Monument Rome* (1995)
43. G. Allesandrini, M. Aglietto, V. Castelvetro, F. Ciardelli, R. Peruzzi, L. Toniolo, J. Appl. Polym. Sci. **76**, 962 (2000)
44. O. Chiantore, M. Lazzari, Polymer **42**, 17 (2001)
45. L. Toniolo, T. Poli, V. Castelvetro, A. Manariti, O. Chiantore, M. Lazzari, J. Cult. Herit. **3**, 309 (2002)
46. G.C. Borgia, M. Camati, F. Cerri, P. Fantazzinim, F. Piacenti, Stud. Conserv. **48**, 217 (2003)
47. A. Tsakalof, P. Manoudis, I. Karapanagiotis, I. Chryssoulakis, C. Panayiotou, J. Cult. Herit. **8**, 69 (2007)
48. L. D'Arienzo, P. Scarfato, L. Incarnato, J. Cult. Herit. **9**, 253 (2008)
49. S. Nilpairach, S.T. Dubas, JMMM **18**, 33 (2008)
50. P.N. Manoudis, A. Tsakalof, I. Karapanagiotis, I. Zuburtikudis, C. Panayiotou, Surf. Coat. Technol. **203**, 1322 (2009)
51. P. Kotlik, *Stavební Materiály Historických Objektů: Materiály, Koroze, Sanace* (ICT Prague, Praha, 1999)
52. V. Schütznerová-Havelková, Bull. Eng. Geol. Environ. **19**, 374 (1979)
53. Compendium of RILEM Technical Recommendations, E&FN Spon (1994)
54. M.D. Murray, B.W. Darvell, J. Phys. D, Appl. Phys. **23**, 1150 (1990)
55. R.N. Wenzel, Ind. Eng. Chem. **28**, 988 (1936)
56. A.B.D. Cassie, S. Baxter, Trans. Faraday Soc. **40**, 546 (1944)
57. D. Quéré, Physica A **313**, 32 (2002)
58. R.E. Johnson, R.H. Dettre, Adv. Chem. Ser. **43**, 112 (1964)
59. M. Morra, E. Occhiello, F. Garbassi, Langmuir **5**, 872 (1989)